INTERNATIONAL JOURNAL OF AUTOMOTIVE SCIENCE AND TECHNOLOGY

2025, VOL. 9, NO:1, 12-25 www.ijastech.org e-ISSN: 2587-0963

The Impact of Temperature and Ageing on LFP Electric Vehicle Batteries: A Comprehensive Modelling Study

Benan Serarslan[1*]

[1.] *Department of Automotive Technologies, Ege University, Izmir, 35100, Turkiye*

Abstract

For several years now, electric cars (E-cars) have increasingly come into the public spotlight. This technology aims to provide alternatives to conventional vehicles with internal combustion engines while creating independence from politically unstable oil-producing countries. Another significant reason for this trend is the reduction of CO_2 emissions to counteract the associated climate change. When powered by renewable energy sources such as wind or solar energy, E-cars theoretically avoid most of the CO_2 emissions. However, from a consumer perspective, E-cars currently have two main disadvantages, such as high acquisition costs and limited range. Due to these two factors, it became imperative to be able to get accurate information about the batteries' state, age, and range. Therefore, this article presents the main influential factors on vehicle range and a comprehensive study of different types of state of art modeling methods. The methodologies with their challenges and the necessity of using the relevant modeling methodology are described. Furthermore, experimental findings after 365 days are presented, using 60 Ah battery cells, to investigate different kinds of aging influence with various parameters like ambient temperature, charging current and depth of discharge.

Keywords: Batteries; Lithium-ion battery; Modelling; Temperature; EV

Research Article

History
Received 21.09.2024
Revised 25.10.2024
Accepted 10.12.2024

Contact
* Corresponding author
Benan Serarslan
benan@dr.com
Address: Department of Automotive Technologies, Ege University, Izmir, 35100, Turkey

***To cite this paper*:** Serarslan, B. The Impact of Temperature and Ageing on LFP Electric Vehicle Batteries: A Comprehensive Modelling Study. International Journal of Automotive Science and Technology. 2025; 9 (1): 12-25. https://doi.org/10.30939/ijastech..1519778

1. Introduction

The rise of electric vehicles (EVs) represents a pivotal shift towards sustainable transportation. Central to the performance and longevity of EVs are their batteries, which are highly susceptible to temperature fluctuations. Understanding the intricate relationship between temperature and EV batteries is crucial for optimizing their performance and ensuring their long-term viability. This essay explores the influence of temperature on EV batteries, drawing insights from state-of-the-art research findings to reveal the underlying mechanisms and implications. A battery system's selection and size depend on the vehicle's requirements. A hybrid vehicle can refer to a wide variety of vehicle concepts. Here are a few classifications of vehicle concepts. The classifications of different car manufacturers are remarkably similar. Overviews have been given by [1-4]. Figure 1 compares all types of electrified vehicles with respect to the energy and power demand. Fuel-cell electric vehicles are not mentioned here explicitly. However, the battery sizing and requirements are typically quite similar to those of full hybrid electric vehicles mentioned in Figure 1.

According to [5] the term "lithium-ion batteries" encompasses a wide range of material combinations used to construct these batteries. The characteristics of lithium-ion batteries, including power, lifespan, performance at low and high temperatures, and safety, are highly dependent on the specific materials used. The electrode design allows optimization towards high-power or high- energy cells. According to Ragone (A performance comparison plot that evaluates different energy storage devices. The x-axis represents the specific power, measured in W/kg, while the y-axis represents the specific energy, measured in Wh/kg.) plot of various (specification at cell level) battery technologies, lithium-ion battery cells achieve the highest gravimetric energy and power densities of all commercially available rechargeable batteries, [5]. Using titanate instead of carbon for the negative active material can achieve very long lifetimes and high safety levels. However, this choice significantly reduces energy density, [6]. A lithium-ion battery (often called Li-ion battery or LIB) is a type of rechargeable battery that uses the reversible intercalation of *Li+* ions into electronically conducting solids to store energy. Compared to other commercial rechargeable batteries, Li-ion batteries are characterized by [7]:

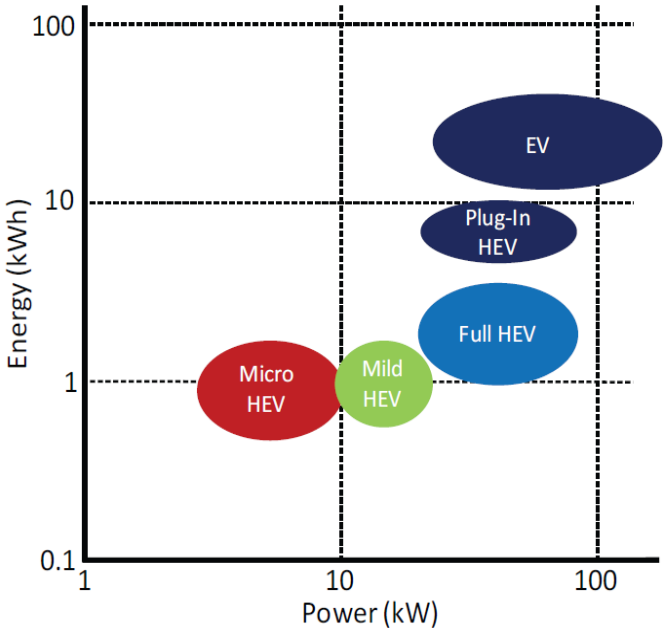

Figure 1. Battery energy and power demands for various types of electrified vehicles (based on market observations, [5]).

- Higher specific energy
- Higher energy density
- Higher energy efficiency
- Longer cycle life
- Longer calendar life

Significant advancements in lithium-ion battery properties have occurred since the mass production of Sony camcorders in 1991. Within the next 30 years, their volumetric energy density increased threefold while their cost dropped tenfold, [8]. These batteries have enabled portable consumer electronics, laptops, cellular phones, and electric cars, contributing to what is known as the e-mobility revolution. They are also widely used for grid-scale energy storage, military applications, and aerospace. Different chemistries of lithium-ion batteries exist, including lithium cobalt oxide (LiCoO2), lithium iron phosphate (LiFePO4), lithium manganese oxide (LiMn2O4 spinel or LMR-NMC), and lithium nickel manganese cobalt oxide (LiNiMnCoO2 or NMC). Each chemistry offers specific advantages and trade-offs, [9]. The invention and commercialization of lithium-ion batteries have had a profound impact on technology and society, recognized by the 2019 Nobel Prize in Chemistry, [9]. These batteries continue to play a crucial role in our daily lives and the transition toward cleaner energy sources, [10]. Despite some advantages of NMC (Nickel Manganese Cobalt) batteries, LFP (Lithium Iron Phosphate) batteries still excel in much longer cycle life than NMC batteries, wider temperature range tolerance and in power capability, delivering higher charging speed performance, [11] and [12].

2. Battery-design, Electrochemistry and the Impact of Temperature and Aging on Batteries

Let's explore the working principle of a lithium-ion battery. These batteries are widely used in various devices, including mobile phones, laptops, and electric vehicles. The following sections describe how they work.

2.1. Battery components

A lithium-ion battery consists of several individual cells connected to each other. Each cell contains three main parts, [13] and [14]: Positive Electrode (Cathode): This electrode is typically made of lithium-metal oxide, such as lithium-cobalt oxide (LiCoO2). It supplies lithium ions (Li+).

Negative Electrode (Anode): The anode usually contains a lithium- carbon compound, allowing for easy movement of lithium ions in and out of its structure.

Liquid Electrolyte: The electrolyte facilitates the movement of lithium ions between the electrodes.

Moreover, there are components like so-called "current collectors", which are conductive foils at each electrode of the battery that are connected to the terminals of the cell. The cell terminals transmit the electric current between the battery, the device, and the energy source that powers the battery. Lastly the "separator", a porous polymeric film that separates the electrodes while enabling the exchange of lithium ions from one side to the other, [9], [15]. For an illustration of the components mentioned, one can refer to [15].

2.2. Electrochemistry

Inside the battery, oxidation-reduction (Redox) reactions occur. Reduction takes place at the cathode (positive electrode). Cobalt oxide (CoO2) combines with lithium ions (Li+) to form lithium-cobalt oxide (LiCoO2):

$$(CoO^2 + Li^+ + e^- \rightarrow LiCoO^2) \quad (1)$$

Oxidation occurs at the anode (negative electrode).

The graphite intercalation compound (LiC_6) forms graphite (C_6) and releases lithium ions:

$$(LiC^6 \rightarrow C^6 + Li^+ + e^-) \quad (2)$$

The overall reaction during discharging (left to right) and charging (right to left) is:

$$(LiC^6 + CoO^2 \rightleftarrows C^6 + LiCoO^2) \quad (3)$$

During the recharging process positively charged lithium ions (Li+) move from the negative anode to the positive cathode through the electrolyte. The electrical current flows from the current collector through the device being powered (e.g., cell phone, computer) to the negative current collector. The separator prevents the flow of electrons inside the battery.

In summary, lithium-ion batteries store and release energy through the movement of lithium ions between the cathode and anode, enabling the devices we rely on daily, [14-15].

2.3. Temperature effects on EV battery performance and case studies

Temperature exerts a significant influence on the electrochemical processes occurring within EV batteries, thereby impacting their performance, efficiency, and lifespan. Extreme temperatures, both hot and cold, can have detrimental effects on battery health.

Recent researches by [13], [16] and [17] highlight the accelerated degradation of lithium-ion batteries, the main battery technology in EVs, at elevated temperatures. These studies demonstrate that prolonged exposure to temperatures above 40°C leads to increased capacity fade and impedance rise, compromising the battery's performance and longevity. Furthermore, high temperatures promote the formation of damaging side reactions, such as lithium plating and electrolyte decomposition, intensifying degradation mechanisms.

Conversely, cold temperatures slow down the electrochemical reactions within EV batteries, resulting in decreased capacity and power output. [18] explains the effects of sub-zero temperatures on lithium-ion batteries, revealing reduced ionic conductivity and slowed-down kinetics, which translate to reduced performance and range in EVs operating in cold climates. Sections 2.3.1 and 2.3.2 give examples of how low and high temperatures affect the aging of the batteries and the charging efficiency of EVs.

2.3.1. Battery aging and degradation

Accelerated Aging

High operating temperatures accelerate battery aging. Charging under elevated temperatures leads to degradation. EV batteries must operate therefore within optimal temperature ranges to maximize lifespan, [19].

Lithium Plating

Low temperatures cause ions to flow more slowly through battery cells. Consequently “lithium plating” occurs, disrupting energy flow and reducing power and range, [20].

2.3.2. Range and charging efficiency

Range Reduction

Cold weather negatively impacts EV range. Chemical reactions within the battery slow down at lower temperatures, affecting capacity. AAA tested EVs in -6.66°C (20°F) weather and found that temperature alone could reduce range by 10-12%. When climate control is used, range loss can amplify to 40%. EV drivers need to be aware of weather conditions, especially during trips, [21].

Charging Time

Cold temperatures increase impedance, leading to longer charging times. Battery conductivity and diffusivity decrease, affecting charging efficiency. Hence, EVs should be above freezing point temperature before charging to optimize performance, [1], [14], [21].

3. Modeling a Lithium-Ion Battery Cell

Lithium-ion batteries are the workhorses behind our portable electronics, electric vehicles, and renewable energy systems. Understanding their behavior and accurately modelling their performance is crucial for optimizing battery-powered systems. In this section, the principles of modelling lithium-ion battery cells, the significance of accurate models, and common approaches used in the field are explored. Battery models have become an indispensable tool for the design of battery-powered systems. Their uses include, [22]:

Battery Characterization

The initial stage in developing a precise battery model involves constructing and parameterizing an equivalent circuit that accurately represents the battery's nonlinear characteristics. Engineers use measurements performed on battery cells of the same type to determine dependencies on temperature, state of charge (SoC), state of health (SoH), and current I.

State-of-Charge (SoC) Estimation

Battery models help develop algorithms for estimating SoC. Modern battery chemistries require sophisticated approaches like Kalman filtering due to flat OCV-SoC discharge signatures.

Degradation Considerations

Batteries experience degradation over time as a result of calendar life and the process of charge-discharge cycles. Models assist in developing battery management strategies that account for degradation.

Real-Time Simulation

Hardware-in-the-loop testing of battery management systems (BMS) relies on accurate battery models. A model designed for system-level development can be reused for real-time simulation.

3.1. Equivalent circuit models

For the modelling of the equivalent circuit part of the batteries the following basics of the circuit should be considered.

Ohmic Resistance in a Lithium-Ion Battery Cell

The ohmic resistance in a lithium-ion battery cell arises from the sum of various resistances. These include the resistances of the metallic conductors, the resistance of the active material, and the electrolyte resistance. Notably, the electrolyte resistance (also known as the ionic resistance) constitutes the largest portion of the ohmic resistance and increases as the temperature decreases. Additionally, the conductivity of the active material depends on the state of charge of the lithium-ion battery cell. To determine the ohmic resistance of a lithium-ion battery cell, a current step is applied at the input, and the incoming voltage step is measured at the output. The quotient of voltage (U) and current (I) yields the ohmic resistance, denoted as R_i, [23]:

$$R_i = U/I \quad (4)$$

Charge Carrier Transit Resistance and Double-Layer Capacitance

When a charge passes between the electrode and the electrolyte, there is a transition from electrical to ionic conduction. The resulting overpotential during this charge transfer is influenced by the charge carrier transit resistance, [23]. At the interface between the electrode and the electrolyte, charge carriers with different polarizations face each other. Physically, this region behaves like a capacitor. The capacity of this capacitor is also known as the double-layer capacitance, [23]. Although the double-layer capacitance does not directly cause the overpotential, it does influence it. Consequently, the entire charge transfer reaction can be represented as a first-order time constant (RC circuit), [23].

Both the charge carrier transit resistance and the double-layer capacitance occur at both electrodes of a lithium-ion battery cell. Therefore, these effects can be modelled using two series-connected parallel RC circuits. The time constants of the two RC circuits may differ according to [23].

Solid-State Diffusion

Solid-state diffusion refers to the movement of ions within a solid material. In the context of batteries, it occurs at the interface between the electrode and the electrolyte. The working principle can be described as following, [13], [24]:

• Ion Consumption or Generation: As ions flow between the electrode and the electrolyte during charge and discharge, they are either consumed or generated. This process creates a concentration gradient within the electrolyte, directed toward the separator, [13].

• Driving Force: Diffusion: Diffusion is the driving force behind ion transport. It ensures that ions move from regions of higher concentration to lower concentration. The Fick's laws describe this diffusion process mathematically.

• Temperature and Geometry: Besides temperature, the geometry of the solid body also plays a crucial role in determining the rate of diffusion. Researchers consider both factors when modelling and optimizing battery performance.

In summary, solid-state diffusion is fundamental to ion transport in batteries, influencing their overall behavior and efficiency. For further details, refer to [23].

3.1.1. Rint-model

There are a number of thermo-electric models in the literature that can be used to describe the behavior of a lithium-ion battery cell. In [25], a total of five electrical models of a lithium-ion battery cell are described, which explain the electrical behavior in a lithium-ion battery cell in different ways:

- Rint-Model,
- RC-Model,
- Thévenin-Model,
- PNGV-Model,
- DP-Model (Double-Polarization-Modell)

The R_{int} model was developed and tested by the National Renewable Energy Laboratory (NREL) in the mid-1990s [26]. In the R_{int} model, the lithium-ion battery cell is represented by an ideal DC voltage source U_{oc} and a charge or discharge resistance (R_{ch} and R_{dch} respectively), Figure 2.

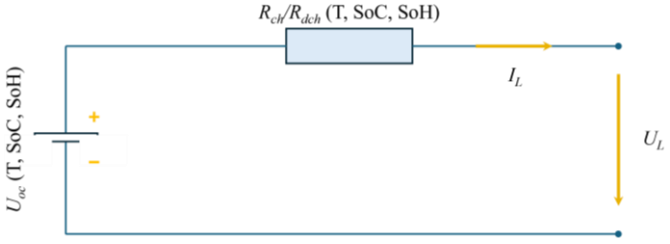

Figure 2. R_{int} model of a lithium-ion battery cell

The ideal DC voltage source is a function of the temperature T, state of charge SoC and state of health SoH. The internal resistance is also a function of T, SoC, SoH and the charge or discharge current I_L. If a charging resistor R_{ch} is used, the lithium-ion battery cell is charged by the current I_L. When discharging, the discharge resistor R_{dch} is used [26].

Therefore, the terminal voltage U_L is described by:

$$U_L = U_{oc} - R_{ch/dch} \cdot I_L \quad (5)$$

Accordingly, SoC is described by the Eq. (6).

$$SoC = \frac{C_N - \int_0^t i_L dt}{C_N} \quad (6)$$

where, C_N represents the nominal capacity and i_L represents the current drawn from or supplied to the lithium-ion battery cell over time. During the discharge process, the current is positive and during the charging process, it is negative.

The SoH of the lithium-ion battery cell describes the decrease in cell capacity due to calendar and cyclic aging. The SoH also describes the health of the lithium-ion battery cell in terms of charging and discharging resistance.

3.1.2. RC-model

The RC model was developed by the company Saft. This model consists of two capacitors (C_c, C_b) and three resistors (R_t, R_e, R_c), Figure 3. The capacitor C_b has a very large capacity (in farads) and represents the ability of a lithium-ion battery cell to store electrical charge in chemical form. The capacitor C_c has a significantly lower capacity (in farads) compared to C_b. The capacitor C_c represents the surface effects such as the chemical reactions and solid-state diffusion effects and associated time constants of the system. The state of charge (SoC) of the lithium-ion battery cell can be determined via the voltage at the capacitor C_b, [25] and [26]. The resistors R_t, R_e and R_c are called terminating-, end- and capacitor-resistors, [25].

The following equations can describe the electrical behavior of the circuit, [27]:

$$\begin{bmatrix}\dot{U}_b\\ \dot{U}_c\end{bmatrix}=\begin{bmatrix}\frac{-1}{C_b(R_e+R_c)} & \frac{1}{C_b(R_e+R_c)}\\ \frac{1}{C_c(R_e+R_c)} & \frac{-1}{C_c(R_e+R_c)}\end{bmatrix}\begin{bmatrix}U_b\\ U_c\end{bmatrix}+\begin{bmatrix}\frac{-R_c}{C_b(R_e+R_c)}\\ \frac{-R_e}{C_c(R_e+R_c)}\end{bmatrix}[I_L] \quad (7)$$

$$[U_L]=\begin{bmatrix}\frac{R_c}{R_e+R_c} & \frac{R_e}{R_e+R_c}\end{bmatrix}\begin{bmatrix}U_b\\ U_c\end{bmatrix}+\begin{bmatrix}-R_t & \frac{-R_eR_c}{R_e+R_c}\end{bmatrix}[I_L] \quad (8)$$

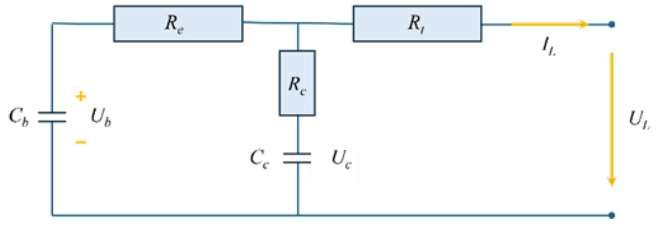

Figure 3: RC model of a lithium-ion battery cell

3.1.3. Thévenin-model

The Thévenin model is an extension of the R_{int}-model. The Thévenin model uses the R_{int}-model as a basis and extends it by a parallel R_C element that is connected in series, Figure 4. "The equivalent-capacitance C_{thn} is used to describe the transient response during charging and discharging. U_{thn} is the voltages across C_{thn}. Lastly, I_{thn} is the outflow current of C_{thn}", [27].

With RC element (R_{Thn}, C_{Thn}) the dynamic processes in the lithium-ion battery cell can be described better, [27]. The lithium-ion battery cell parameters are determined by examining the lithium-ion battery cell under different loads. A well-known approach to obtain the corresponding lithium-ion battery cell parameters is electrochemical impedance spectroscopy (EIS), [28].

The electrical behavior of Thévenin models can be described by the following equations:

$$U_{Thn}=\frac{\hat{U}}{R_{Thn}C_{Thn}}+\frac{I_L}{C_{Thn}} \quad (9)$$

$$U_{Thn}=\frac{\hat{U}}{R_{Thn}C_{Thn}}+\frac{I_L}{C_{Thn}} \quad (10)$$

3.1.4. PNGV-model

The PNGV model (Partnership for a New Generation of Vehicles) is based on the Thévenin model. As an extension to the Thévenin model, another capacitor with the voltage U_d is connected between the ohmic resistor and the RC element, Figure 4. This capacitor represents the temporal change in the open circuit voltage when the load current changes, [25]. The following equations can describe the electrical behavior of PNGV-Models:

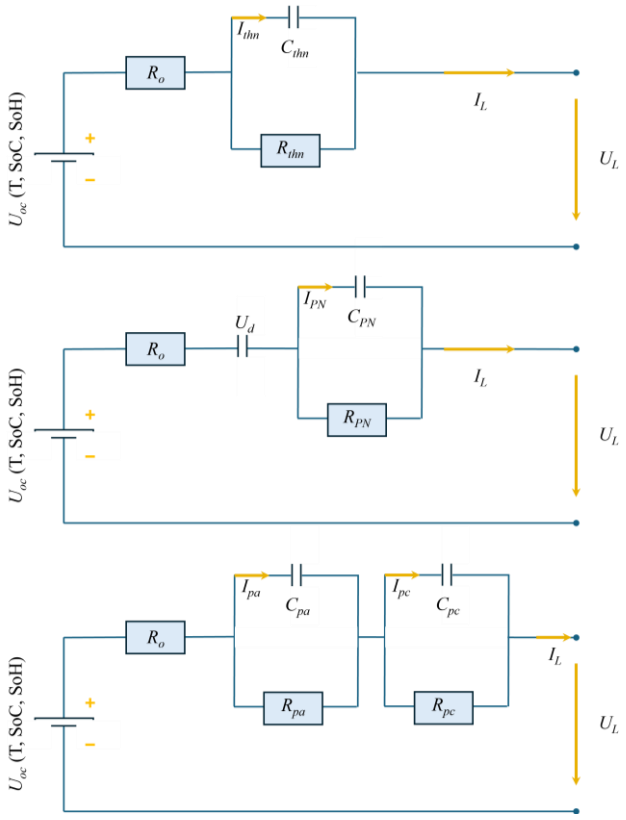

Figure 4: Thévenin, PNGV and DP models (from Top to Bottom) of a lithium-ion battery cell

$$\dot{U}_d=U'_{oc}\cdot I_L \quad (11)$$

$$\dot{U}_{PN}=-\frac{\dot{U}_{PN}}{R_{PN}C_{PN}}+\frac{I_L}{C_{PN}} \quad (12)$$

$$U_L=U_{oc}-\dot{U}_d-\dot{U}_{PN}-I_LR_0 \quad (13)$$

3.1.5. Double-polarization-model

The double polarization model (DP model) consists of an ideal voltage source U_{oc}, an ohmic internal resistance R_0 and two RC parallel elements R_{pa} and C_{pa} as well as R_{pc} and C_{pc} connected in series, Figure 4.

The ohmic internal resistance R_0 represents the resistances of the electrodes, the electrolyte, and the active material.

Both RC parallel elements represent the charge transfer resistance and the double layer capacitance at the anode and the cathode. The time constants of the two RC elements may be different, [36].

The electrical behavior of the DP model is described by the following equations:

$$\dot{U}_{pa}=\frac{-U_{pa}}{R_{pa}C_{pa}}+\frac{I_L}{C_{pa}} \quad (14)$$

$$\dot{U}_{pc} = \frac{-U_{pc}}{R_{pc}C_{pc}} + \frac{I_L}{C_{pc}} \quad (15)$$

$$U_L = U_{oc} - \dot{U}_{pa} - \dot{U}_{pc} - I_L R_0 \quad (16)$$

The individual values of the resistors and capacitors for the DP model can be determined using electrochemical impedance spectroscopy (EIS). In EIS on battery cells, a sinusoidal alternating current $\hat{I}$ is fed to the test object as an input variable and the voltage response $\hat{U}$ is measured as an output variable. In addition, a direct current can be superimposed to set the operating point of the test object.

The complex impedance of the test object can be calculated using the discrete Fourier transformation, see Eq. (17), [41].

$$\bar{Z} = \frac{\bar{u}}{\bar{\imath}} = \frac{\hat{U} \cdot e^{j(2\pi f t + \varphi_u)}}{\hat{I} \cdot e^{j(2\pi f t + \varphi_i)}} = \frac{\hat{U}}{\hat{I}} \cdot e^{j(\varphi_u - \varphi_i)} \quad (17)$$

Using EIS, dynamic models of battery cells can be developed, and the condition of different battery cells can be determined, and aging effects identified, [38], [42].

According to [38], all models show a very small deviation compared to the voltage measurement on the test bench. The DP and Thévenin models describe the behavior of the cell voltage most accurately, with a maximum error of 0.4 to 0.5%. The RC and PNGV models have a voltage deviation of 1 to 2%. The R_{int}-model has the largest deviation at 2.8%.

In conclusion, by modelling RC elements in the RC, Thévenin, PNGV and DP models, the dynamic processes such as charge transfer, double layer capacity and solid-state diffusion processes in the battery cell are described, [36]. The R_{int}-model does not have any RC elements and therefore cannot depict the dynamic processes mentioned above. However, the calculation time of the R_{int}-model is shorter compared to other cell models, which is also reflected in shorter cycle times in real-time capability.

3.2. Thermal modelling

Thermal effects significantly impact battery performance and safety. A thermal model considers heat absorption or dissipation through, [43]:

- Conduction: Heat transfer within the battery.
- Convection: Heat exchange with the surrounding environment.
- Radiation: Thermal radiation.
- Internal Heat Source: Heat generated during operation.
- Parameters like thermal conductivity (λ), thermal capacity C_t, and emissivity coefficient (ε) are essential for accurate thermal modelling.

Furthermore, the following aspects explain the importance of thermal modelling and its challenges:

Temperature Impact on Battery Performance

Battery performance is highly temperature-dependent regarding the following aspects:

- Capacity: Battery capacity decreases at low temperatures due to sluggish chemical reactions.
- Lifetime: Elevated temperatures accelerate degradation, reducing battery lifespan.
- Safety: Excessive heat can lead to thermal runaway and safety hazards.

Key Aspects of Thermal Modelling

- Heat Generation: During charge and discharge, batteries generate heat due to internal resistance and irreversible reactions. Heat is also produced during fast charging or high current draw. Accurate modelling requires understanding of these heat sources.
- Heat Dissipation Mechanisms: Batteries dissipate heat through various mechanisms like conduction, convection, etc. like described above. Modelling these mechanisms helps predict temperature distribution.
- Thermal Resistance and Capacitance: Equivalent thermal circuits represent batteries. Thermal resistance R_t describes how easily heat flows through the battery and thermal capacitance. C_t represents the battery's ability to store heat. The boundary conditions for those thermal modelling assumptions are i.e. external factors (ambient temperature, cooling systems) affect battery temperature. Modelling boundary conditions ensures accurate predictions.

Challenges in Thermal Modelling

- Nonuniform Temperature Distribution: Batteries have varying temperature profiles due to spatial and temporal variations. Modelling must account for this nonuniformity.
- Transient Effects: Rapid charge/discharge cycles cause transient temperature changes. Transient modelling captures dynamic behavior.
- Coupling with Electrochemical Models: Combining thermal and electrochemical models is complex. Accurate predictions require solving coupled equations.

In summary, thermal modelling ensures efficient battery design, optimal operation, and safety. Researchers and engineers continue to refine models to address real-world challenges in battery technology.

3.3. Aging types and modelling

A cell model for electrical behavior was discussed in the previous section. The chemical behavior of a lithium-ion battery cell with respect to aging is discussed in this section, [31]. "The reasons for battery aging, such as lithium deposition and the formation of Solid Electrolyte Interphase (SEI), are widely studied in the literature", [32].

There are two forms of degradation associated with aging, loss of capacity and increased resistance. A classical empirical model was developed to model these two consequences. These models focus on simulating the aging effects with constant conditions (SoC, temperature, current) in the long run, [33], [34]. These models are usually accurate over a long period of time at steady conditions. The objective of this aging model is to simulate instantaneous degradation of a lithium-ion battery, unlike most existing models that cannot simulate degradation over a short period of time (a few seconds), nor under evolving conditions. This is because the current and the temperature of the battery pack supply energy to the powertrain at varying rates, [35].

A cycle aging model and a calendar aging model are represented by two different equation packages. The aging model switches from one aging mode to another depending on if the vehicle is being driven or parked. Additionally, the aging factors depend on temperature, whereas temperatures around 20°C are optimum for storage and operation of the batteries.

3.3.1. Calendar ageing

Basically, a distinction is made between calendar and cyclic aging to describe the aging of lithium-ion battery cells. Both mechanisms lead to a decrease in the capacity and performance of the lithium-ion battery cell, [49]. The decrease in performance is due to the increase in charging and discharging resistance. According to [50] the main reasons for the aging of lithium-ion battery cells are:

- Change in the morphology of the anode/cathode,
- Reduction in the active surface of the anode/cathode,
- Binder degradation at the anode/cathode,
- Irreversible intercalation of lithium at the anode (graphite),
- Corrosion of the metallic conductor (copper) of the anode,
- Electrolyte contamination,
- Separator abrasion,
- Reduction in the porosity of the separator.

According to [49], [51] and [44], calendar ageing is a temperature-sensitive chemistry process that can be described by the Arrhenius law. The usual equations Eq. (18) and Eq. (19) were put into their integral form to determine the instantaneous ageing, [51]. To switch from a time scale in days to a time scale in seconds, in order to calculate the degradation effects in periods of time in the order of seconds, the equations Eq. (18) and Eq. (18) were modified into Eq. (20) and Eq. (21) respectively as follows:

$$Q_{loss}^{cal} = A_c \cdot e^{-\frac{E_{a_C}}{K_T}} \cdot t^Z \tag{18}$$

$$R_{rise}^{cal} = A_r \cdot e^{-\frac{E_{a_r}}{K_T}} \cdot t^Z \tag{19}$$

$$Q_{loss}^{cal} = \sqrt{\int_0^D \frac{1}{86400} \cdot {A_c}^2 \cdot e^{-\frac{2E_{ac}}{K_T}} dt} \tag{20}$$

$$R_{rise}^{cal} = \sqrt{\int_0^D \frac{1}{86400} \cdot {A_r}^2 \cdot e^{-\frac{2E_{ar}}{K_T}} dt} \tag{21}$$

Q_{loss}^{cal} is the capacity loss and R_{rise}^{cal} is the resistance increase due to calendar ageing. A_c and A_r are the pre-exponential factors of the capacity loss and of the resistance increase due to calendar ageing respectively. E_{ac} and E_{ar} are the activation energies of the capacity loss and of the resistance increase due to calendar ageing respectively. K is the Boltzmann-constant and T is the temperature. D is the test duration in seconds, t the time and z the power factor varying between 0.5 and 1. In the model, z is set to 0.5, [32].

With the tests performed by [39], calendar ageing data of three different types of Li-ion battery cells (18650 LFP, NMC and NCA cells) were obtained for a duration of 300 days. For each type of battery, the tests were performed on identical cells coming from the same production batch under different conditions, at 3 different temperatures (25°C, 40°C and 50°C) and 16 different SoC levels, leading to 48 different calendar ageing conditions tested for each technology, [32].

The capacity loss and resistance increase were obtained for every SoC level for the 3 different temperatures. A three linear equations system was then obtained and solved using the least squares method to determine values for A and E_a.

The results are presented in Figure 5. The evolution of the activation energies for capacity loss and the resistance increase, E_{ac} and E_{ar}, are shown in Figure 5b and Figure 5e respectively, [39].

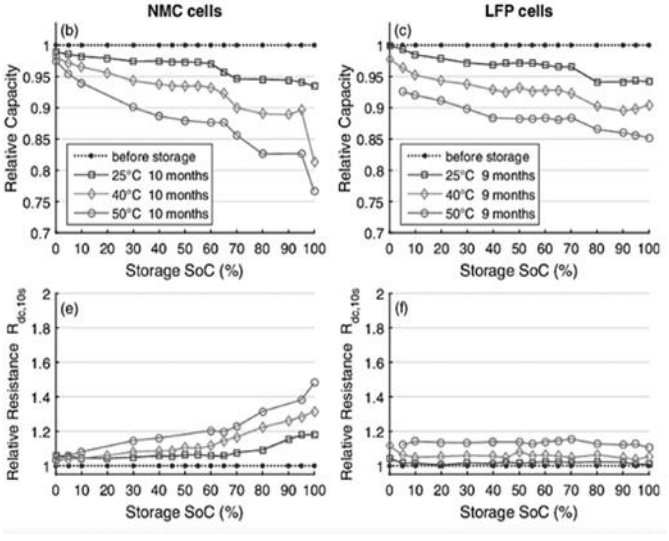

Figure 5. Battery degradation after ca. 9–10 months of storage at various SoCs and different temperatures: (b-c) capacity fade; (e-f) rise of internal resistances, [39].

3.3.2. Cycle ageing

The SoH of a lithium-ion battery cell is determined not only by the calendar aging, but also by the cyclic aging. Cycling aging happens when the battery undergoes charging and discharging cycles. This aging process is affected by various mechanisms, including parasitic physicochemical transformations, which degrade the battery's energy capacity and power (impedance) capabilities, [38]. The stress factors for cyclic aging are temperature, depth of discharge DOD and current. Suppose the cyclic aging or the cyclic aging factor per cycle is known at the beginning of the battery cell tests. In that case, the aging of the lithium-ion battery cell for additional cycles can be estimated using a straight-line equation.

In the literature, cycle ageing is often described as a function of the number of cycles, [35], [34] and [32]. In this case, the simulation time also needs to be expressed in function of time, [32].

It was assumed that a cycle of cyclic ageing contains a complete discharge and a complete charge and that the difference between the charge and the discharge was neglectable. So, it was considered that the same amount of positive and negative current (stress) has the same influence on the chemical degradation of the battery.

Therefore, the ageing behavior of one cycle can be distributed over each instant. It is considered that for each cycle, the real-time is equal to 2 times the real capacity C_{real} divided by the current I (once during charge, once during discharge), as shown in the Eq. (22):

$$\mathrm{ds} = 2\frac{\mathrm{C_{real}}}{\mathrm{I}}3600\mathrm{dt} \tag{22}$$

Then, to change from a number of cycles to a time in seconds, the following variable change must be carried out:

$$t = \int_0^{S_{fini}} \frac{I}{7200\mathrm{C_{real}}}\,ds \tag{23}$$

For the cycle ageing, the rate of capacity loss and resistance increase is influenced not only by the temperature but also by the current level. Therefore, the rate of charge and discharge C-rate has been added into the calculation. The loss of capacity and the increase of resistance are calculated through the Eq. (24) and Eq. (25) as follows, [44]:

$$Q_{loss}^{cyc} = 2A_c \cdot e^{\left(\frac{-E_{a_c}+B_c \cdot C_{rate}}{R \cdot T}\right)} \cdot t^Z \tag{24}$$

$$R_{rise}^{cyc} = A_r \cdot e^{\left(\frac{-E_{a_r}+B_r \cdot C_{rate}}{R \cdot T}\right)} \cdot t^Z \tag{25}$$

Q_{loss}^{cyc} is the capacity loss and R_{rise}^{cyc} is the resistance increase due to cycle ageing. A_c and A_r are the pre-exponential factors of the capacity loss and of the resistance increase for the cycle ageing respectively. E_ac and E_ar are the activation energies of the capacity loss and of the resistance increase due to cycle ageing respectively. *C*-rate is the cycling rate. B_c and B_r are the current accelerating factors, that adjust the impact of the *C*-rate, of the capacity loss and the resistance increase respectively. R is the perfect gas constant; t is the number of cycles and z is a power factor varying between 0.5 and 1. From the data given in the reference [35], it was observed that cycle ageing behaviors evolved linearly with the number of cycles, so z was set to 1. After applying the variable change described in Eq. (23), the capacity loss and the resistance increase are then expressed under their integral form as followed in Eq. (26) and Eq. (27), [32]:

$$Q_{loss}^{cyc} = \int_0^{S_{fini}} A_c e^{\left(\frac{-E_{a_c}+B_c \cdot C_{rate}}{R \cdot T}\right)} \frac{I}{3600\mathrm{C_{real}}}\,ds \tag{26}$$

$$R_{rise}^{cyc} = \int_0^{S_{fini}} A_r e^{\left(\frac{-E_{a_r}+B_r \cdot C_{rate}}{R \cdot T}\right)} \frac{I}{3600\mathrm{C_{real}}}\,ds \tag{27}$$

where, s_{fini} is the cycle duration.

The parameters identification was carried out based on the data published by [40]. They found the activation energy E_{ac} and the acceleration factor A_c for a simpler cycle ageing model which doesn't consider the regime impact. They discovered that A_c = A_r = 11443 and E_{ac}= E_{ar} = 42570 J·mol^{-1}. Those values were reused as predefined parameters in this model. Regarding the values of B_c and B_r, they were calibrated from the data published by [47] using the least squares method. They investigated the cycle ageing behavior of a LCO cell at different cycling rates (0.5C, 0.8C, 1C, 1.2C 1.5C) at a given temperature of 25°C. From the Eq. (24) and Eq. (25), it is observed that when the regime and the temperatures are fixed, the capacity loss and the resistance increase are linear as a function of time (or number of cycles). The data from [35] allow us to determine the values of K_c and K_r, which are the slopes of the evolution of capacity and resistance respectively. They are defined as follows, [32]:

$$K_c = 2A_c \cdot e^{\left(\frac{-E_{a_c}+B_c \cdot C_{rate}}{R \cdot T}\right)} \tag{28}$$

$$K_r = A_r \cdot e^{\left(\frac{-E_{a_r}+B_r \cdot C_{rate}}{R \cdot T}\right)} \tag{29}$$

According to [30], the proposed calendar and cycle aging models imply that the degradation rate remains constant as long as the cycles are consistent. However, lithium-ion battery degradation experiments reveal a different reality. The degradation rate of lithium-ion batteries is non-linear with respect to the number of cycles. In battery aging tests, as depicted in Figure 6, we observe the following trends:

- Early Cycles: During the initial cycles, the degradation rate is significantly high. See region A.
- Later Cycles: As the cycles progress, the degradation rate stabilizes. See region B and C.

- End of Life (EoL): Approaching the end of life, the degradation rate increases rapidly. See region D.

This observation underscores that the degradation rate of lithium-ion batteries is intrinsically tied to their current life state. [54] shows the same picture like in Figure 6, but with a much higher degradation rate in region D and suggests that battery manufacturers do not publicize data reports for region D. Moreover, unfortunately, there are also not many tests or simulations publicly available in the literature for this region D, but mostly in region A and B only.

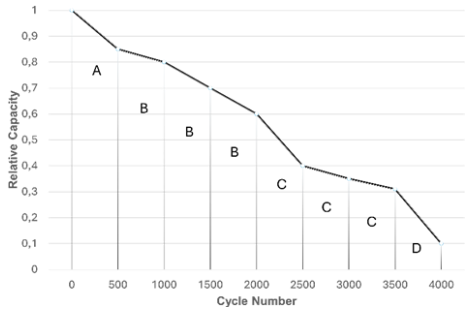

Figure 6. General capacity degradation behavior of lithium-ion batteries.

To achieve a more accurate aging modelling one can refer to [30]. They did not use the least squares method but added the factor of active lithium ions left. Hence, they managed to add some non-linearity of the degradation rate as can be seen from the Figure 7 and [30]. Note that the non-linearity strongly depends on the chemistry of the battery. For the modelling details and constraints please refer to [30].

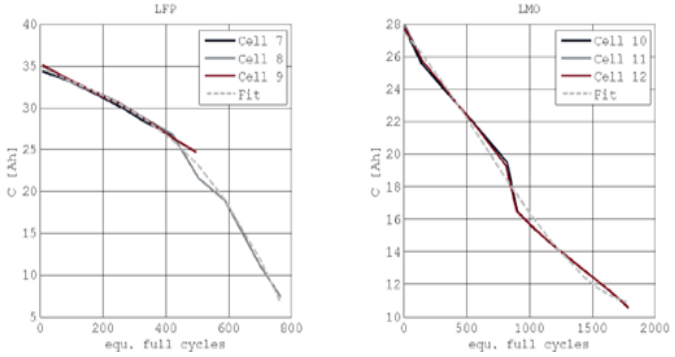

Figure 7. Evolution of the capacity during cycling of the different chemistries; LFP and LMO, [30].

Lastly, according to [38], accelerated ageing tests were performed on lithium-ion cells at 60°C to assess the impact of different SoC levels on calendar ageing and to examine the interactions between cycling and calendar ageing in electric vehicle applications. The results indicate that cycling and calendar ageing interact in complex ways, making it challenging to model both processes simultaneously. In the same research article, it is stated that the cycling ageing results are more challenging to analyze due to numerous factors and their interactions. Because during these tests, calendar ageing overlaps with cycling ageing. To isolate the calendar ageing component within the cycling ageing data, they employed a cumulative damage approach.

3.3.3. Temperature ageing

The ideal temperature for any battery is around 25°C (77°F), which is considered as room temperature. Manufacturer datasheets usually specify the cycle life based on this temperature. However, operating a battery at higher temperatures, especially near its maximum limit, accelerates its ageing process. The ageing factor value measures the time spent at temperatures above room temperature, with the rate of ageing increasing as the temperature rises. The formula to calculate this factor is $F_t = h \times (0.002t^2 + 0.03t)$, where "$t$" is the temperature rise above 25°C and "h" is the battery's calendar life in hours, [42], [16].

The stress model for temperature is based on the Arrhenius equation, which describes how the rate of a chemical reaction depends on temperature [16].

$$S_T(T) = e^{k_T \cdot (T - T_{ref}) \frac{T_{ref}}{T}} \quad (30)$$

where:

$S_T(T)$ is the temperature-dependent stress factor, k_T is a constant that represents the temperature sensitivity, T is the absolute temperature, T_{ref} is the reference temperature.

While the Arrhenius equation suggests that the degradation rate decreases as the temperature lowers, this relationship does not apply at low temperatures.

The authors of [17] show that the temperature of 20°C serves as a critical threshold between high and low temperature effects on battery behavior. When the temperature remains above 20°C, the battery's impedance decreases. However, if the temperature drops below 20°C, the impedance increases. Notably, calendar aging test data from this research suggests that the degradation rate at 15°C is smaller than at 25°C.

Experimental results also show that the battery is aging exponentially faster when it spends its life at higher temperatures, Fig8.

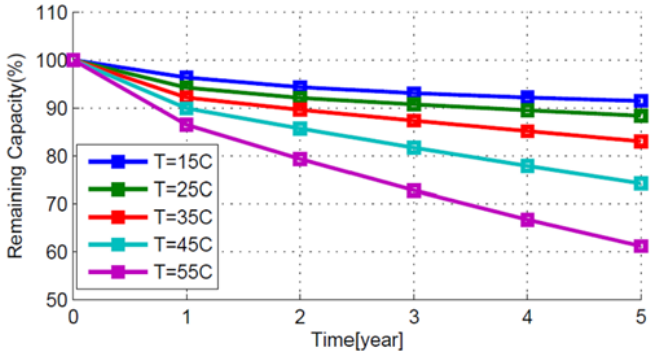

Figure 8. Calendar aging with varying temperature at 50% SoC [42].

4. Research and Tools

Researchers continuously refine battery models to improve accuracy. The first step in the development of an accurate battery model is to build and parameterize an equivalent circuit that reflects the battery's nonlinear behavior and dependencies on temperature, SoC, SoH, and current. These dependencies are specific to each battery's chemistry (see i.e. Section 3.3) and must be determined through measurements conducted on battery cells that are identical to those intended for use with the controller being designed, [43]. Tools like MATLAB&Simulink offer powerful capabilities for battery modelling and simulation, [43]. Academic studies explore nonlinear modelling of lithium-ion battery cells for electric vehicles, [44]. Books like Mathematical Modelling of Lithium Batteries provide in-depth insights, [45].

Briefly, modelling lithium-ion battery cells is a dynamic field with practical implications for energy storage, electric mobility, and sustainability. With advancing technology, accurate models will continue to play a fundamental role in shaping the future of battery-powered systems.

For thermal modelling tools and approaches like following can be considered, [46]:

- Finite Element Analysis (FEA) simulates heat transfer within battery cells and packs. Accounts for geometry, material properties, and boundary conditions.
- Computational Fluid Dynamics (CFD) help to make models fluid flow and heat transfer in battery cooling systems. Useful for electric vehicle battery packs, [47].
- Multiphysics Simulation Tools like ANSYS and MATLAB&Simulink offer multiphysics capabilities for thermal modelling. Furthermore, coupling with electrochemical models is feasible, [46].

In summary, thermal modelling ensures efficient battery design, optimal operation, and safety. Researchers and engineers continue to refine models to address real-world challenges in battery technology.

5. Experimental Setup

The calendar aging assessment of the LFP battery cell involves considering three ambient temperatures (0°C, 25°C, 40°C) and three state of charge ranges (1-0.75 / 0.75-0.5 / 0.5-0.25). Altogether, this leads to a total of nine distinct test series, as illustrated in Table 1. These factors play a crucial role in understanding the behavior and durability of the battery cell over time.

These controlled conditions allow researchers to study the impact of temperature and state of charge on the aging process of the LFP battery cell. Moreover, the cyclic aging of the LFP battery cell is conducted with the following stress factors: temperature (0°C, 25°C, 40°C), discharge current (25 A, 50 A, 100 A), and discharge depth (0.25 / 0.5 / 0.75). This results in a total of 27 test series, as summarized in Table 2.

Table 1: Test series for calendar aging

Test Series #	Ambient Temperature [°C]	State of Charge Range (SoC)
1	0	1.0 - 0.75
2	0	0.8 - 0.5
3	0	0.5 - 0.2
4	25	1.0 - 0.75
5	25	0.8 - 0.5
6	25	0.5 - 0.2
7	40	1.0 - 0.75
8	40	0.8 - 0.5
9	40	0.5 - 0.2

Table 2: Test series for cycle aging

Test Series #	Current [A]	Ambient Temperature [°C]	Depth of Discharge (DoD)
1	0.5	0	0.2
2	1	0	0.2
3	2	0	0.2
4	0.5	0	0.5
5	1	0	0.5
6	2	0	0.5
7	0.5	0	0.75
8	1	0	0.75
9	2	0	0.75
10	0.5	25	0.2
11	1	25	0.2
12	2	25	0.2
13	0.5	25	0.5
14	1	25	0.5
15	2	25	0.5
16	0.5	25	0.75
17	1	25	0.75
18	2	25	0.75
19	0.5	40	0.2
20	1	40	0.2
21	2	40	0.2
22	0.5	40	0.5
23	1	40	0.5
24	2	40	0.5
25	0.5	40	0.75
26	1	40	0.75
27	2	40	0.75

A battery test bench is established to study the calendar and cyclic aging of a 60 Ah LFP battery cell. This setup incorporates water tempering, which is employed to control and regulate the ambient temperature of the battery cell during testing. This arrangement enables the examination of temperature variations on the battery's performance and longevity.

For this purpose, the ratio of irreversible capacity loss $C_{cal,irv}$ and $C_{cyc,irv}$ to the total capacity C is calculated as follows:

$$A_{cal} = C_{cal,irv} / C \quad (31)$$

$$A_{cyc} = C_{cyc,irv} / C \quad (32)$$

6. Results –how to minimize aging of EV LFP Batteries–

6.1. Experimental findings for calendar aging with various temperatures

In Table 3, the values of A_{cal} for all test subjects after 365 days

All measurements to determine A_{cal} were approximated at an ambient temperature of 25°C using the extended Arrhenius equation, see Eq. 30. By maintaining all test subjects at 25°C, a direct comparison between the A_{cal} values can be made.

Table 3: A_{cal} after 365 days

Battery Temp. [°C]	SoC 1-0.75	SoC 0.75-0.5	SoC 0.5-0.25	Sample No:
0	0.036	0.041	0.015	01 || 02 || 03
25	0.043	0.0418	0.032	21 || 22 || 23
40	0.066	0.056	0.034	41 || 42 || 43

It is noticeable that the A_{cal} of the test subjects increases with rising temperature and increasing state of charge range. Thus, please note that sample no 41 has the highest and no 01 the lowest A_{cal} after 365 days.

6.2. Experimental findings for cycle aging with various temperatures and charging currents

Table 4 shows all the test subjects for 1000 charge and discharge cycles each. All test samples approximated by a linear equation at 25°C ambient temperature. Further details can be found in Section 3.3.2. and in [30].

In summary, it can be noted (for most test subjects) the A_{cyc} increases with decreasing temperature, increasing depth of discharge, and increasing load current. It is interesting to see here that calendar and cycle aging behave differently with varying temperatures. Considering both findings for LFP batteries, it can be recommended to keep the batteries at an average ambient temperature of 25°C, recharge after at least reaching 40-50% SoC or below and charge it at a higher charging current wherever/whenever possible.

7. Conclusions and Outlook

In this paper, an overall analysis of different battery modeling methods is described. Furthermore, long-term experimental findings about different kinds of aging are shown with various parameters like temperature, charging current. Multiscale modeling and numerical simulation of rechargeable lithium-ion batteries present several challenges due to their complex behavior and critical role in various applications.

Table 4: A_{cyc} with various temperatures after ca. 2000 cycles

Charging Current [A] at 0°C	DoD 0.25	DoD 0.5	DoD 0.75	Sample No:
25	0.011	0.028	—	04 || 05
50	0.035	0.085	—	54 || 55
100	0.055	—	—	101
Charging Current [A] at 25°C	**DoD 0.25**	**DoD 0.5**	**DoD 0.75**	**Sample No:**
25	0.007	0.003	0.019	25 || 26 || 27
50	0.011	0.030	0.042	75 || 76 || 77
100	0.032	0.036	0.070	125 || 126 || 127
Charging Current [A] at 40°C	**DoD 0.25**	**DoD 0.5**	**DoD 0.75**	**Sample No:**
25	0.045	0.007	0.002	45 || 46 || 47
50	0.001	0.010	0.030	95 || 96 || 97
100	0.020	0.045	0.060	145 || 146 || 147

Let's explore some of these challenges according to [48-50]:

Energy Density

- The energy density is constrained by battery's chemistry, which inherently determines the theoretical maximum energy density.
- Components like thermal management and current collectors contribute to the total weight of the battery system, affecting energy density.

Power Density and Fast Recharge

- High power density is crucial for electric vehicles during regenerative braking or fast recharge.
- Balancing high current densities during recharge and lower densities during discharge is challenging.
- Fundamental battery components (electrodes, separator, and electrolyte) impact power density.

Life, Reliability, and Safety

- Battery lifespan should imply gradual, controlled discharge to mitigate wear and minimize the risk of failure.
- Uneven current density distribution, poor discharge/recharge control, and inadequate thermal management can accelerate wear and elevate failure risks.
- Monitoring the state of health (SoH) and safety risks is essential.

Costs

- Battery manufacturing processes are not as optimized as those for mechanical powertrains.

- Scaling up production can lower costs, but balancing performance and affordability remains a formidable challenge.

Sustainability

- Developing new batteries must consider mining, recycling, pro- duction, and disposal strategies.
- Sustainability is a legal and commercial consideration for manufacturers and automotive companies.

It is shown that different temperatures influence battery performance and life differently. Temperatures below 25°C are good for battery storage (thus mitigating calendar and temperature aging). Whereas temperatures above 25°C are good for vehicle/battery ranges (thus mitigating cycle aging). To simulate these aging factors is challenging because they occur at the same time and hence, they are difficult to separate from each other. Additionally, discharge rates, depth of discharge, and battery chemistry strongly influence the battery's lifespan and performance. For further research, it is recommended to integrate those different models and evaluate the accuracy of the new modeling experimentally with varying discharge rates and depths. Also, an overall simulation analysis and an evaluation of the latest and the most accurate lithium-ion battery models are provided in this paper.

The "ideal" or optimal state of charge (SoC) for a lithium-ion battery is 50%, where the electrochemical processes inside the battery are most stable. Deviation from this midpoint accelerates battery aging, assuming all other parameters are equal. However, this process is highly non-linear, with significant effects becoming noticeable only at the extreme ends of the SoC range over extended periods. Practically, maintaining a battery within a 5%-90% SoC range is almost as beneficial as keeping it at 50%. The most significant impact on SoC aging comes from holding a fully charged battery voltage above its natural resting voltage after charging is complete. Therefore, proper charge termination is crucial for lithium batteries. During charging, the voltage is held higher to facilitate current flow into the battery and overcome internal resistance. However, once charging is finished, the charger must lower the voltage to what is commonly called the Float level, where a fully charged battery can be safely maintained. If the battery is not used for long periods, for optimum storage guidelines, one can refer to [42] and [13].

In summary, it can be stated that there are numerous research studies in scientific literature regarding the thermoelectric modeling of lithium-ion batteries. Many of these studies focus on battery cells with capacities in the single-digit range, covering only a portion of the spectrum of different temperatures to which lithium-ion batteries are exposed. No studies are known up to date that describe a thermoelectric model of a 60 Ah LFP battery cell, including both calendar and cyclic aging, at different temperatures of 0°C, 25°C, and 40°C, as well as for different currents of 25A, 50A, and 100A, while investigating real-time capability.

As part of this work, both a model and a battery test bench were created, which are very advantageous for further investigations in terms of their flexibility. On the one hand, this model can be used to determine the service life of an LFP battery down to the cell level if the performance profile is known. This means that the model created, and the battery test bench can be used not only for vehicles, but also for all other applications in which these LFP battery cells are installed.

Conflict of Interest Statement

There is no conflict of interest in this study.

Nomenclature

EV	Electric vehicle
HEV	Hybrid electric vehicle
$Li+$	Lithium ion
$LiClO4$	Lithium perchlorate
$LiPF6$	Lithium hexafluorophosphate
LFP	Lithium iron phosphate $LiFePO_4$
NMC	Lithium nickel manganese cobalt oxides $LiNiMnCoO_2$
PNGV	Partnership for a New Generation of Vehicles
RC	Resistor capacitor
Rint	The internal resistance
SoC	State of charge
SoH	State of health

References

[1] Ntombela M, Musasa K, Moloi KA. comprehensive review for battery electric vehicles (bev) drive circuits technology, operations, and challenges. World Electric Vehicle Journal. 2023;14(7). https://doi.org/10.3390/wevj14070195

[2] Lukic SM, Cao J, Bansal R. Energy storage systems for automotive applications. IEEE Transactions on Industrial Electronics. 2008;55(6):2258–2267. https://doi.org/10.1109/TIE.2008.918390

[3] Oman H, Gross S. Electric–vehicle batteries. IEEE Aerospace and Electronic Systems Magazine. 1995;10(2):29–35. https://doi.org/10.1109/62.350734

[4] Karden E, Ploumen B, Fricke B, Miller T, Snyder K. Energy storage devices for future hybrid electric vehicles. Journal of Power Sources. 2007;168(1):2–11. https://doi.org/10.1016/j.jpowsour.2006.10.090

[5] Budde-Meiwes H, et al. A review of current automotive battery technology and future prospects. Journal of Automobile Engineering. 2013;227:761–776. https://doi.org/10.1177/0954407013485567

[6] Zelinsky MA, Koch JM, Young KH. Performance comparison of rechargeable batteries for stationary applications. Batteries. 2017; 4(1):2–6. https://doi.org/10.3390/batteries4010001

[7] Xing Y, Ma EW, Tsui KL, Pecht M. Battery management systems in electric and hybrid vehicles. Energies. 2011;4(11):1840–1857. https://doi.org/10.3390/en4111840

[8] Gerssen-Gondelach SJ, Faaij APC. Performance of batteries for

electric vehicles on short and longer term. Journal of Power Sources. 2012;212:111–129. https://doi.org/10.1016/j.jpowsour.2012.03.085

[9] Habib AA, Motakabber SMA, Ibrahimy MI. A comparative study of electrochemical battery for electric vehicles applications. In: 2019 IEEE International Conference on Power, Electrical, and Electronics and Industrial Applications (PEEIACON). Dhaka; 2019;2019 November 29;44–46. https://doi.org/10.1109/PEEIACON48840.2019.9071955

[10] Zhou ML, Wie L, Wen JB. The parameters matching and simulation of pure electric vehicle composite power supply based on cruise. Applied Mechanics and Materials. 2014;602:2836–2839. https://doi.org/10.4028/www.scientific.net/AMM.602-605.2836

[11] Ognjen P, Veljko R, Željko P, Snežana A, Vladimir M. Testing of NMC and LFP Li-ION cells for surface temperature at various conditions. Case Studies in Thermal Engineering. 2024;61:104930. https://doi.org/10.1016/j.csite.2024.104930

[12] Fallah Seyedeh & Fitzpatrick Colin. Is shifting from Li-ion NMC to LFP in EVs beneficial for second-life storages in electricity markets? The Journal of Energy Storage. 2023;68:107740 https://doi.org/10.1016/j.est.2023.107740

[13] Edge JS, et al. Lithium ion battery degradation: what you need to know. Physical Chemistry Chemical Physics. 2021;23(14):8200–8221. https://doi.org/10.1039/D1CP00359C

[14] Megahed S, Scrosati B. Lithium-ion rechargeable batteries. Journal of Power Sources. 1994;51(1-2):79–104. https://doi.org/10.1016/0378-7753(94)01956-8

[15] Tosun E, Keyinci S, Yakaryılmaz AC, Yıldızhan Ş, Özcanlı M. Evaluation of Lithium-ion Batteries in Electric Vehicles. IJASTECH.2024;8(3):332-40. https://doi.org/10.30939/ijastech..1460955

[16] Xu B, Oudalov A, Ulbig A, Andersson G. Modeling of lithium-ion battery degradation for cell life assessment. IEEE Transactions on Smart Grid. 2016;9(2):1131–1140. https://doi.org/10.1109/TSG.2016.2578950

[17] Lam L, Bauer P, Kelder E. A practical circuit-based model for li-ion battery cells in electric vehicle applications. In: 2011 IEEE 33rd International Telecommunications Energy Conference (INTELEC). 2011;2016 October 9–13. https://doi.org/10.1109/INTLEC.2011.6099803

[18] Garud KS, Le DT, Seong-Guk H, Nghia-Huu N, Moo-Yeon L. A review of advanced cooling strategies for battery thermal management systems in electric vehicles. Symmetry. 2023;15(7). https://doi.org/10.3390/sym15071322

[19] Wu S, Xiong R, Li H, Nian V, Ma S. The state of the art on preheating lithium–ion batteries in cold weather. Journal of Energy Storage. 2020;27(101059). https://doi.org/10.1016/j.est.2019.101059

[20] Lin X, Khosravinia K, Hu X, Li J. Lithium plating mechanism, detection, and mitigation in lithium-ion batteries. Progress in Energy and Combustion Science. 2021;87(100953). https://doi.org/10.1016/j.pecs.2021.100953

[21] Steinstraeter M, Heinrich T, Lienkamp M. Effect of Low Temperature on Electric Vehicle Range. World Electric Vehicle Journal. 2021; 12(3):115. https://doi.org/10.3390/wevj12030115

[22] Schaltz E. Electric Vehicles-Modelling and Simulations. InTech; 2011. http://dx.doi.org/10.5772/20271

[23] Jossen, A. Moderne Akkumulatoren richtig einsetzen. 1st ed.; Reichardt Verlag; 2006. ISBN 978-3939359111.

[24] Wu Y, Liu Y, Feng X, Ma Z. Smart solid-state interphases enable high-safety and high-energy practical lithium batteries. Advanced Science. 2024;11(22). https://doi.org/10.1002/advs.202400600

[25] He H, Xiong R, Fan J. Evaluation of lithium-ion battery equivalent circuit models for state of charge estimation by an experimental approach. Energies. 2011;582–598. https://doi.org/10.3390/en4040582

[26] Johnson VH, Pesaran AA, Sack T. Temperature-dependent battery models for high-power lithium-ion batteries. In: 17th Annual Electric Vehicle Symposium. 2000;2000 October 15-18;3–14. https://www.nrel.gov/docs/fy01osti/28716.pdf

[27] Hongwen H, Xiong R, Jinxin F. Evaluation of lithium-ion battery equivalent circuit models for state of charge estimation by an experimental approach. Energies. 2011;(4):582–598. http://dx.doi.org/10.3390/en4040582

[28] Jadidi Y. Advanced State Prediction of Lithium-ion Traction Batteries in Hybrid and Battery Electric Vehicle Applications; vol. 51 of Schriftenreihe des Instituts für Verbrennungsmotoren und Kraftfahrwesen der Universität Stuttgart. expert verlag ein Imprint von Narr Francke Attempto Verlag. 2011; ISBN 9783816930631.

[29] Proakis J, Manolakis D. Digital Signal Processing: Principles, Algorithms and Applications. 3rd ed.; New Jersey, USA: Prentice-Hall, Inc.2006;680–689; ISBN 978-0133737622.

[30] Popp H, Attiaa J. Lifetime analysis of four different lithium ion batteries for (plug–in) electric vehicle. In: Transport Research Arena. Paris, 2014;5:5–7 https://www.researchgate.net/publication/301788355

[31] Al-Zareer M, Dincer I, Rosen M. Heat transfer modeling of a novel battery thermal management system. International Journal of Heat and Mass Transfer. 2018;73:1–14. https://doi.org/10.1080/10407782.2018.1439237

[32] Soloy A, Bartoli T, Haidar F. Modelling and fault diagnosis of lithium-ion battery for electric powertrain. International Journal of Automotive Science And Technology. 2023;7(3):234–247. https://doi.org/10.30939/ijastech..1295130

[33] Amine K, Liu J, Belharouak I. High-temperature storage and cycling of c-lifepo4/graphite li-ion cells. Electrochemistry Communications. 2005;7(7):669–673. https://doi.org/10.1016/j.elecom.2005.04.018

[34] Jalkanen K, et al. Cycle aging of commercial nmc/graphite pouch cells at different temperatures. Applied Energy. 2015;154:160–172. https://doi.org/10.1016/j.apenergy.2015.04.110

[35] Jiang Y, Zhang J, Zhang C, Ma W, Jiang Z, Gao Y. Lithium-ion battery aging mechanisms and life model under different charging stresses. Journal of Power Sources. 2017;356:103–114. https://doi.org/10.1016/j.jpowsour.2017.04.084

[36] Schmalstieg J, Käbitz S, Ecker M. A holistic aging model for

li(nimnco)o2 based 18650 lithium-ion batteries. Journal of Power Sources. 2014;257:325–334. https://doi.org/10.1016/j.jpowsour.2014.02.012

[37] Jin X, Vora A, Hoshing V, Saha T. Applicability of available li-ion battery degradation models for system and control algorithm design. Control Engineering Practice. 2018;71:1–9. https://doi.org/10.1016/j.conengprac.2017.10.002

[38] Redondo-Iglesias E, Venet P, Pelissier S. Calendar and cycling ageing combination of batteries in electric vehicles. Microelectronics Reliability. 2018;88-90:1212–1215. https://doi.org/10.1016/j.microrel.2018.06.113

[39] Keil P, et al. Calendar aging of lithium-ion batteries. Journal of The Electrochemical Society. 2016;163(9). https://doi.org/10.1149/2.0411609JES

[40] Yuksel T, Michalek J. Development of a simulation model to analyze the effect of thermal management on battery life. In: SAE 2012 World Congress Exhibition. 2012; 2012-01-0671 https://doi.org/10.4271/2012-01-0671

[41] Spotnitz R. Simulation of capacity fade in lithium-ion batteries. Journal of Power Sources 2003;113(1):72–80. https://doi.org/10.1016/S0378-7753(02)00490-1

[42] Roy PK, Shahjalal M, Shams T, Fly A, Stoyanov S, Ahsan M, Haider J. A Critical Review on Battery Aging and State Estimation Technologies of Lithium-Ion Batteries: Prospects and Issues. Electronics. 2023;12(19):4105. https://doi.org/10.3390/electronics12194105

[43] Ma S, Jiang M, Tao P, Song C, Wu J, Wang J, Deng T, Shang, W. Temperature effect and thermal impact in lithium-ion batteries: A review. Progress in Natural Science: Materials International. 2018;28(6):653–666. https://doi.org/10.1016/j.pnsc.2018.11.002

[44] Khalfi J, Boumaaz N, Soulmani A. Nonlinear modeling of lithium-ion battery cells for electric vehicles using a hammerstein–wiener model. Journal of Electrical Engineering Technology. 2020;16:659–669. https://doi.org/10.1007/s42835-020-00607-2

[45] Hariharan KS, Tagade P, Ramachandran S. Mathematical Modeling of Lithium Batteries. 1st ed.; Springer Cham; 2018.

[46] Marcello T, Lalo M, et al. LIONSIMBA: A Matlab Framework Based on a Finite Volume Model Suitable for Li-Ion Battery Design, Simulation, and Control. Journal of The Electrochemical Society. 2016;163(7). https://doi.org/10.1149/2.0291607jes

[47] Yin L, Geng Z, Björneklett A, Söderlund E. An integrated flow–electric–thermal model for a cylindrical li-ion battery module with a direct liquid cooling strategy. Energy Technology. 2022;10(8). https://doi.org/10.1002/ente.202101131

[48] Franco AA. Multiscale modelling and numerical simulation of rechargeable lithium ion batteries: concepts, methods and challenges. The Royal Society of Chemistry. 2013;3:13027–13058. https://doi.org/10.1039/C3RA23502E

[49] Ramadesigan V, et al. Modeling and simulation of lithium-ion batteries from a systems engineering perspective. The Electrochemical Society, Inc. 2012;159(3). https://doi.org/10.1149/2.018203jes

[50] Zhu W, Zhou P, Ren D, Yang M, Rui X, et al. A mechanistic calendar aging model of lithium-ion battery considering solid electrolyte interface growth. International Journal of Energy Research. 2022;46:15526–15529. https://doi.org/10.1002/er.8249